Journal of Zhejiang University-SCIENCE A (Applied Physics & Engineering)
ISSN 1673-565X (Print); ISSN 1862-1775 (Online)
www.zju.edu.cn/jzus; www.springerlink.com
E-mail: jzus@zju.edu.cn

Metro train-induced vibrations on historic buildings in Chengdu, China*

Meng MA[†1, 2], Valéri MARKINE[2], Wei-ning LIU[1], Yang YUAN[1], Feng ZHANG[1]

([1]*School of Civil Engineering, Beijing Jiaotong University, Beijing 100044, China*)

([2]*Section of Road and Railway Engineering, Department of Design and Construction, Delft University of Technology, Delft 2600GA, the Netherlands*)

[†]E-mail: mameng_02231250@163.com

Received Apr. 3, 2011; Revision accepted Aug. 18, 2011; Crosschecked Sept. 8, 2011

Abstract: In this paper, the vibration influence on a monument caused by Chengdu Subway Line 2 is analyzed. Due to its elaborate and unique design, both structural and architectural damages should be avoided. First, the allowable root mean square (RMS) velocity at the foundation of the monument is derived and a site measurement is performed to obtain the background vibrations induced by road traffic. In addition, a train-track coupled model and 3D tunnel-soil-structure coupled finite element models are built to predict the dynamic response of the monument. Prediction models are checked by site measurement in Beijing Subway Line 5. Different kinds of fasteners and train speeds are compared and discussed as well. Results show that: (1) At a train speed of 72 km/h, all the traffic vibrations exceed the low limit no matter what kind of fastener is used, which is mainly due to the contribution of road traffic. Slowing down train speeds can cause effective vibration attenuation; (2) Vibrations drop dramatically with the train speed from 65 to 58 km/h. When the train speed is lower than 58 km/h, vibrations are lower than allowable value even if the contribution of road traffic is considered.

Key words: Traffic vibrations, Historic buildings, Vibration prediction, Numerical simulation
doi:10.1631/jzus.A1100088 **Document code:** A **CLC number:** U231; TB533.2

1 Introduction

With the rapid development of the urban rail transit system and the construction of buildings, ground-borne vibrations induced by subway trains and their influence on building structures have become major environmental concerns in urban areas. Generally, it is extremely rare for vibrations from train operations to cause any sort of building damage, even minor cosmetic damage (Heckl *et al.*, 1996). However, there is sometimes a concern regarding long-term vibration effects on historic buildings located near the subway lines. Traffic vibrations are usually low, but lasting, which could lead to potential damage, like building material fatigue and foundation settlement to historic buildings. For structures that have suffered from weathering, desquamation, or have cracks, even low velocities could give rise to fatigue damage with frequent occurrences.

In Europe, damage to some historic buildings caused by road traffic has been reported by Bata (1971) and Clemente and Rinaldis (1998). To protect heritage buildings against traffic-induced vibrations, many studies have been performed in Great Britain, Italy, and Spain (Ellis, 1987; Bazaco *et al.*, 1995; Chiostrini *et al.*, 1995; Sanò *et al.*, 1998; Crispino and D'Apuzzo, 2001; Pau and Vestroni, 2008). In China, there has been doubt that the rapid development of desquamation and cracks of frescoes and sculpture are related to the traffic vibrations in the Longmen Grottoes and Dunhuang Grottoes. Some

* Project supported by the National Natural Science Foundation of China (No. 51008017), and the Fundamental Research Funds for the Central Universities (Nos. 2009JBM074 and 2009JBM075), China

studies have indicated that, by the vibration of railway and highway, the disasters to the Longmen Grottoes from vibration in the last 30 years has exceeded the total experienced in the prior 1000–1500 years (Zhang, 2002; Lei *et al*., 2009). To understand further how to protect historic buildings against subway train-induced vibrations, the route design and isolation methods have been studied for Beijing Lines 4, 5, 6, 8, and 9 and the Straight Railway Line and Xi'an Lines 2 and 6 (Liu *et al*., 2007; Jia *et al*., 2008; Ma *et al*., 2009).

Note that there are two kinds of building damage: structural and architectural. The former will destroy some structure elements and endanger the safety of these buildings, while the latter will just cause cosmetic damage or cracks which, however, are also not allowed for those with superior artistic value or historic value. In this paper, a case study on the effects of vibration from Chengdu Subway Line 2 is presented. Both site measurements and numerical simulations are performed to analyze the effect of vibration from road traffic and subway trains.

2 Problem outline

2.1 Description of historic buildings

The historic monument is located in the People's Park, center of Chengdu City, China (Fig. 1). It was built to remember the martyrs struggling for defending railway sovereignty in the Autumn of Xinhai Year (1911). This brick-masonry structure, with a height of about 30 m, was built in 1913, and was listed as a State Protected Historic Site. There are fine handwritings and reliefs in the four faces. Due to its elaborate and unique art design, both structural and architectural damages should be avoided. Recently, Chengdu Subway Line 2 was built close to it. The distance between the monument and new subway station is about 50 m.

2.2 Vibration criteria for historic buildings

As vibration velocity can reflect the intensity of potential damage to structures, and the peak value has a direct relationship to the fatigue damage to buildings, peak particle velocity (PPV) is often used to evaluate the effects of vibration on building structures. For modern steel structures or reinforced structures, it is believed that a PPV lower than 10 mm/s will rarely cause any sort of building damage. For historic buildings and memorials, the criteria are usually stricter, from 3 to 10 mm/s PPV, depending on local codes, which are summarized by Ma *et al.* (2009). Numerous measurements show that typical ground vibration levels from underground tunnels lie in the range of 0.05–1.00 mm/s, lower than the values in the codes mentioned above, but they remains the possibility of damages to historic buildings. That is, the PPVs between 3 and 10 mm/s do not generally consider architectural damage, but rather structural damage.

Fig. 1 Monument to the martyrs in the autumn of Xinhai Year (1911), in the struggle for defending railway sovereignty

The Chinese National Code (GB/T 50452-2008) gives a criterion of 0.10–0.75 mm/s, which is now one of the strictest allowable values in the world and could be used to evaluate architectural damage. In this code, the fatigue limit is used to fix the allowable velocities. When the cyclic stress is lower than the limit, the materials and structures are unlikely to be destroyed by fatigue. In this case study, for the brick-masonry structure listed as a State Protected Historic Site, the allowable horizontal PPV at the top of the monument is 0.15–0.25 mm/s, according to GB/T 50452-2008. Nevertheless, the vibration responses on the top of the monument are not easy to measure. In order to obtain a predictable response with different kinds of traffic, the allowable root-mean-square (RMS) velocity at the bottom of the

building is more useful.

First, the relation between the PPV at the top and bottom can be expressed as

$$V_{\max} = V_r D = V_r \sqrt{\sum_{j=1}^{n} (\gamma_j \beta_j)^2}, \quad (1)$$

where $V_{\max}$ is the horizontal PPV at the top of the building, V_r is the horizontal PPV at the foundation of the building, γ_j and β_j are the participating factor and dynamic amplifying factor of the jth vibration mode, respectively, j=1,2…,n, and D is a dynamic factor of the ratio of $V_{\max}$ and V_r. By numerical modeling, which will be discussed in Section 3.2, the factor D is about 4.5–5.5. Therefore, the allowable PPV at the foundation V_r that can be calculated by Eq. (1) is 27.27–55.56 μm/s.

Second, the crest factor provides the possibility to change PPV into RMS velocity. The traffic-induced vibrations can be seen as a stationary narrow-band Gaussian process, whose mean value μ approaches 0 and the variance is σ^2. Therefore, the RMS velocity of a group of sample data of vibration signal is

$$\begin{aligned} \mathrm{RMS} &= \sqrt{\frac{1}{n}\sum_{i}^{n} x^2} = \sqrt{E(x_i^2)} \\ &= \sqrt{D(x_i) + [E(x_i)]^2} \\ &= \sqrt{\sigma^2 + \mu^2} = \sigma, \end{aligned} \quad (2)$$

where n is the number of signal sample x, and E and D are the functions of expected value and variance, respectively. That is, RMS is just the standard deviation σ of this signal. For the Gaussian distribution, the probabilities of sample data within $3n\sigma$, $4n\sigma$, and $5n\sigma$ can be obtained by

$$\begin{cases} p(3\sigma) = 99.730020\%, \\ p(4\sigma) = 99.993666\%, \\ p(5\sigma) = 99.999943\%. \end{cases} \quad (3)$$

This means, if the vibration responses obey the Gaussian distribution absolutely, a crest factor larger than 3 yields a probability over 99%. Suppose subway trains operate 10 h every day and the sampling frequency is 1280 Hz, the values of crest factor data larger than 4 and 5 are about 4600 and 41, respectively. For important historic buildings, the former value is still too large, but the latter is acceptable. In order to define a conservative allowable RMS velocity, the crest factor in this study is defined as 5. Therefore, the maximum RMS velocity in the horizontal direction at the ground of the building (Point 1 in Fig. 2) should be 5.45–11.11 μm/s, which is regarded as the vibration criteria in this case study.

2.3 Site measurement for background vibrations

The arterial street lays on the northeast of the monument with a distance of about 80 m. Site measurements have been performed to obtain an understanding on the background vibration mainly caused by road traffic. Fig. 2 shows the positions of the accelerometers. Point 1 is at the ground of the monument, Point 2 is on the pedestal of the monument, while Point 3 and Point 4 are on the ground nearby. At each measurement point, accelerometers both on the vertical direction and horizontal direction parallel to the street, are installed.

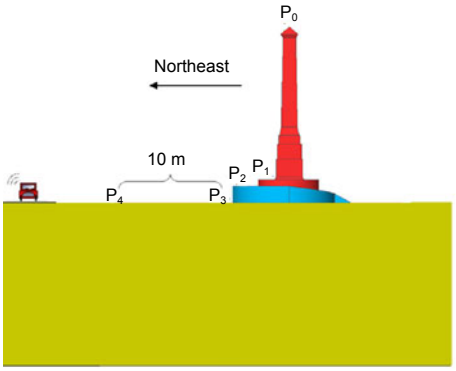

Fig. 2 Schematic of measurement points
P_0–P_4 represent Points 0–4

The measurement configuration consists of eight LC0130 piezoelectric accelerometers, and an INV3020A high-precision portable data acquisition system. The data acquisition hardware was connected to a PC via a USB interface. All these instruments were calibrated by Measure Center of China Aerospace Science and Technology and National Institute of Measurement & Testing Technology. Velocities can be calculated by integral from acceleration responses. The final average results were based on at least 10 records, which are listed in Table 1.

Table 1 Background vibration velocities by measurement

Direction (Point)	PPV (mm/s)		RMS velocity (μm/s)	
	Horizontal	Vertical	Horizontal	Vertical
1	0.0201	0.0454	4.1266	10.0833
2	0.0199	0.0405	4.8068	9.0926
3	0.0380	0.0431	7.1167	9.2366
4	0.0516	0.0444	9.4248	10.2490

2.4 Characteristics of tunnel and soil

According to the geologic survey report of Chengdu Subway Line 2, the strata are simplified to four layers from top to bottom in this area. The dynamic soil characteristics are listed in Table 2. E_d and ν_d are dynamic elastic modulus and dynamic Poisson's ratio, respectively, and H and ρ are the thickness and density of each soil layer, respectively.

Table 2 Dynamic soil characteristics

Layer	Soil type	H (m)	E_d (MPa)	ν_d	ρ (kg/m^3)
1	Miscellaneous fill	5.5	150	0.38	1900
2	Loose gravel	5.7	425	0.28	1900
3	Dense gravel	16.4	893	0.27	2200
4	Weathered mud stone	∞	1000	0.35	2350

The Jiangjun Yamen Station near the monument is 138 m long and the embedded depth of the track is about 13 m. It is a double-decked station with island platform. The reinforced concrete lining of the subway has a Young's modulus of 3.5×10^4 MPa, a Poisson's ratio of 0.25, a density of 2500 kg/m^3, and a hysteretic material damping ratio of 0.02.

3 Numerical models

In this section, to study the vibration responses caused by subway trains, a coupled train-track-tunnel-soil-structure model for vibration analysis is built. For the convenience of calculation, it is a simple method wherein the 3D system is simplified into a 2D train-track model and a 3D tunnel-soil-structure model. On one hand, the dynamic effects of moving train loads are mainly on the vertical direction, much larger than those on the horizontal and longitudinal directions. Therefore, in the train-track model, the structure is loaded by vertical loads only and in the horizontal plane the structure properties are symmetric with respect to the track axis. On the other hand, it is not a good idea to simplify a building as a plane-strain problem. The moving effect is important; thus, a 3D tunnel-soil-structure model is employed. As an output of the first 2D model, two groups of moving train forces will be applied on the second 3D model.

3.1 Dynamic train-track models

To obtain the dynamic forces acting in the tunnel-soil-structure models, numerical models are created in the computer software DARTS_NL developed at Delft University of Technology, the Netherlands. DARTS_NL is specialized finite element software for analysis of the dynamic railway vehicle-track interaction. Various track structures such as ballasted track, slab track, and viaduct, can be modelled in DARTS_NL. The software has been successfully used for various railway applications such as optimization of a slab track (Markine *et al*., 2000; 2001), identification of dynamic properties of track components (Markine *et al*., 2003), assessment of various high-speed track structures (Esveld and Markine, 2006; Markine and Esveld, 2007), and analysis of the dynamic forces due to bad welds (Steenbergen, 2008). The main parts of the software and the developed models of subway train-track are described below.

The dynamic analysis of track-vehicle interaction that includes track flexibility can be computationally expensive. In order to reduce the computational effort, the modelling in DARTS_NL is restricted to two dimensions (the vertical and longitudinal directions) while using linear material property elements. A track structure is modelled using a series of alternating hard and soft layers. Each hard layer consists of Timoshenko beam elements, while the elastic layers are represented by distributed spring and damper combinations (Kelvin elements).

Depending on the properties of the finite elements, these layers can be used for modelling various track components, such as rails, rail pads, sleepers, ballast, concrete slabs, subgrade, and foundation piles, etc. By defining the appropriate topology and imposing the necessary boundary conditions, various railway track structures can be modelled.

The dynamic train-track model is schematically shown in Fig. 3. In this model, each vehicle is modeled by a mass-spring system that consists of four

wheels, two bogies, and a car body, all of which are rigid bodies and connected to each other by the primary and secondary suspensions. The track model consists of three hard and three soft layers. The hard layers are modeled as Timoshenko beams, with both bending stiffness and shear stiffness, while the elastic layers are represented by spring-damper combinations. The contact wheel/rail forces are modeled by means of a non-linear Hertzian contact spring (Grassie, 1984):

$$K_{\mathrm{H}}=\sqrt[3]{\frac{6E^2P\sqrt{R_{\mathrm{w}}R_{\mathrm{r}}}}{4(1-\nu^2)^2}}, \tag{4}$$

where P is the static wheel load, R_{w} and R_{r} are the radiuses of the wheel and rail profile, E is the Young's modulus of the wheel and rail material, and ν is Poisson's ratio.

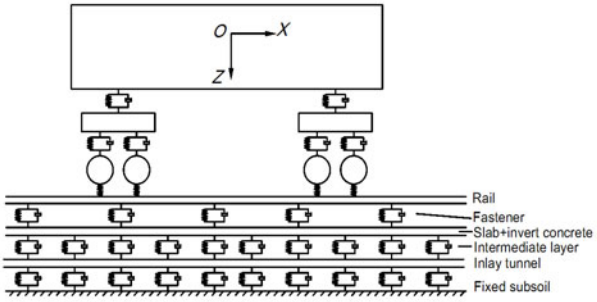

Fig. 3 Schematic of dynamic train-track model

Proper representation of the track geometry in the numerical model is important for realistic simulation of the vehicle-track interaction. Containing both long and short wave irregularities, the rail geometry represents the main source of the dynamic excitations in the vehicle-track system. In DARTS_NL the vertical rail geometry can be defined either as a periodic function or as a numeric data profile obtained from measurements. As there is no existing power spectral density (PSD) of track irregularity for subways in China, in this study, a rail surface data file NSTO_new is employed, which was from the measurement results of a railway line with new rails and with a total length of 1 km (Fig. 4a). Compared with the measured acceleration on the rail in Beijing Subway, here the data from 400 to 750 m of the total 1 km database in the surface file NSTO_new are used.

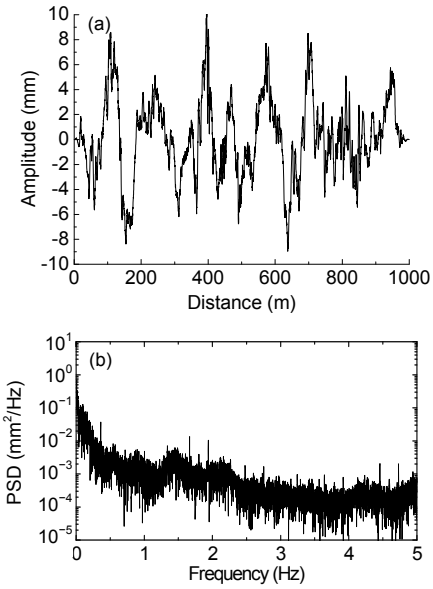

Fig. 4 Surface file NSTO_new of rail geometry profile (a) and average PSD of vertical rail geometry (b)

The size of the integration step is determined by

$$\Delta t \le \frac{\Delta x_{\min}}{v}, \tag{5}$$

where $\Delta x_{\min}$ is the smallest element size, which is 0.1 m; and v is the train speed, here the largest train speed of Chengdu Subway is employed, 20 m/s. Therefore, the integration step $\Delta t \le 0.005$ s. Finally, the step of 0.0032 s is chosen, and then the spectrum of dynamic load are between 0 and 156.25 Hz, which contains main frequencies of ground vibrations caused by train loads.

The dynamic analysis is performed in the time domain following the concept of the displacement method (Zienkiewicz and Taylor, 1988; Kok, 1995). The direct integration process has been used. The main steps in the numerical procedure are:

(1) Assembling the mass $\boldsymbol{M}$, damping $\boldsymbol{C}$ and stiffness $\boldsymbol{K}$ matrixes and the vector of the external forces $\boldsymbol{f}$;

(2) Generation of the equations of motion:

$$\boldsymbol{M}\ddot{\boldsymbol{u}}+\boldsymbol{C}\dot{\boldsymbol{u}}+\boldsymbol{K}\boldsymbol{u}=\boldsymbol{f}; \tag{6}$$

(3) Solution of the equations of motion yielding displacement vector $\boldsymbol{u}$ and acceleration $\ddot{\boldsymbol{u}}$;

(4) Filtering of the obtained displacements

vector $\boldsymbol{u}$ and acceleration $\ddot{\boldsymbol{u}}$ by cutting off the high frequency contributions (optional);

(5) Calculation of responses based on the (filtered) displacements $\boldsymbol{u}$. The responses include: stresses, forces, and bending moments in the rail and rail supports; accelerations of the vehicle; dynamic wheel forces; and contact forces.

Details of the numerical method implemented in the DARTS_NL software can be found in Kok (1995).

3.2 Coupled tunnel-soil-structure finite element models

To predict the vibration response of the monument, the finite element method software MIDAS-GTS was used to build 3D finite element models of tunnel-soil-structure, and subjected to train loads of different kinds of fasteners and different train speeds. According to the shear wave velocity of different soil layers and the excited frequency range, the model takes a dimension of 120 m×60 m×60 m, and the size of elements ranges from 0.5 to 5 m.

The Rayleigh damping can be calculated by

$$\boldsymbol{C} = \alpha \boldsymbol{M} + \beta \boldsymbol{K}, \tag{7}$$

where $\boldsymbol{C}$ is defined as a linear superposition of $\boldsymbol{M}$ and $\boldsymbol{K}$ with the coefficients α and β. The two coefficients can be only defined by the damping ratio of soils and the analysis frequencies. The damping ratios of soil are usually about 0.01–0.3, while those of sand and pebble are much smaller, about 0.004–0.12. According to the lab test for sand pebble in Chengdu area by Wang (2006) and geologic survey report, a constant damping ratio 0.006 is employed here. Therefore, the coefficients can be calculated as α=0.3589 and β=1.82×10^{-5}.

Soils are divided into four layers. The material properties are shown in Table 2. Special viscous-elastic artificial boundary is used to eliminate the reflection of propagation waves. The 3D finite element model is shown in Fig. 5.

3.3 Model checking

In order to check whether the model could predict the vibration response effectively, measurements have been performed in Beijing Subway Line 5, both at the vibration source and on the ground above this metro line.

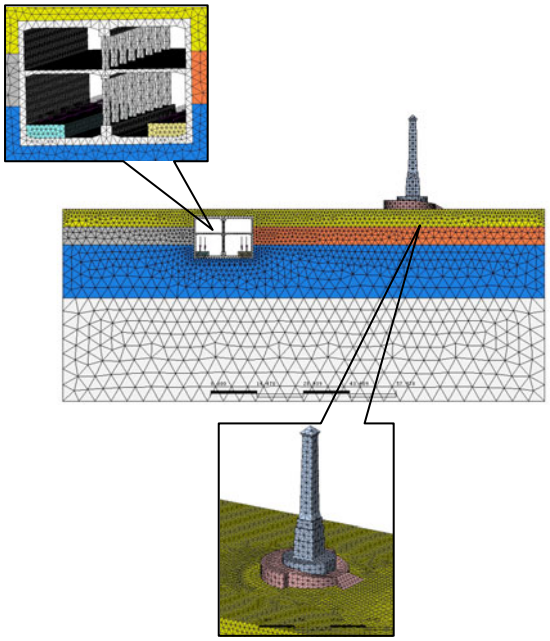

Fig. 5 3D finite element model of subway station, soil and monument

Fig. 6 shows the acceleration sensor on the rail. The dynamic responses and dynamic train loads can be calculated by the train-track model in Section 3.1. Comparing the accelerations between measurement and simulated results in time and frequency domain, we find that the amplitude and the frequency contents are similar, and especially the dominant frequency matches well (Fig. 7).

Fig. 6 An acceleration sensor on the rail

In addition, another ground vibration measurement was performed as well. The measurement point is just above the center of the two tunnel lines (Fig. 8). Another tunnel-soil 3D finite element model was set up for the section of running tunnel. The meshing,

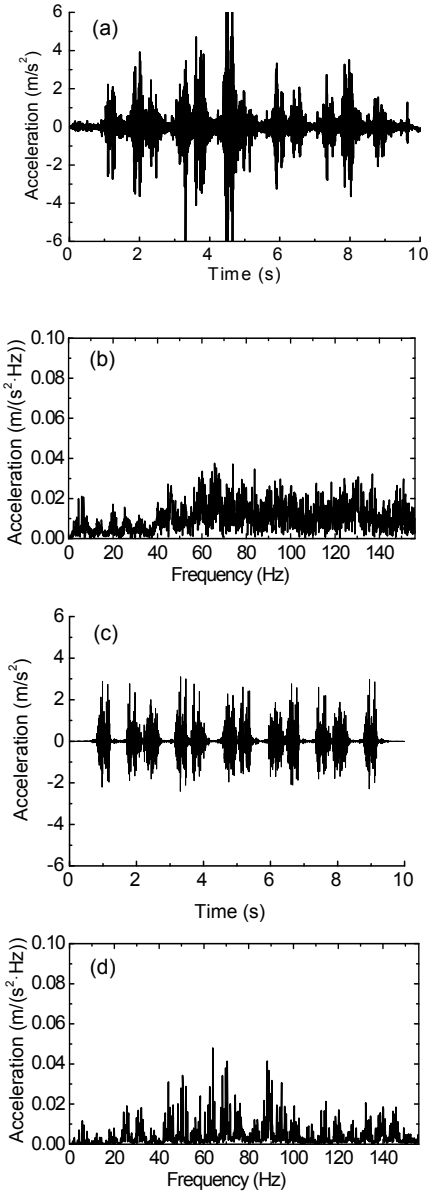

Fig. 7 Time history (a) and frequency spectrum (b) of measured acceleration on the rail; Time history (c) and frequency spectrum (d) of simulated acceleration on the rail

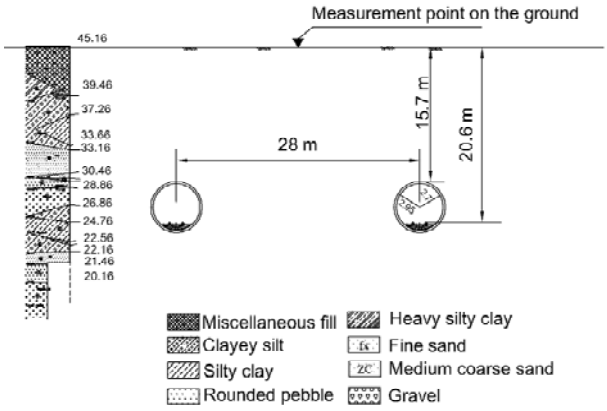

Fig. 8 The soil conditions and site parameters of Beijing Subway Line 5 (unit: m)

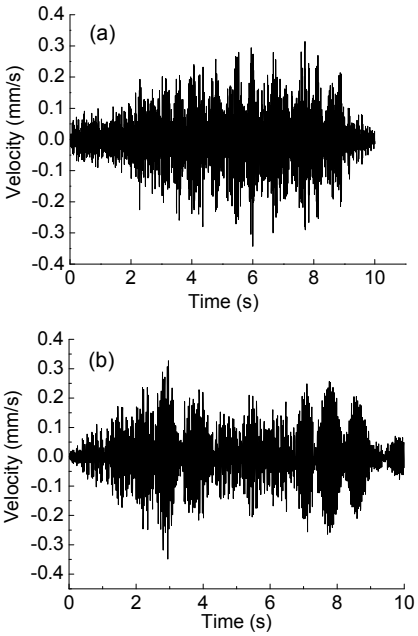

Fig. 9 Measured (a) and simulated (b) ground vibration velocity for Beijing Subway Line 5

damping definition, train load simulation, and boundary conditions are the same as mentioned in Sections 3.1 and 3.2. Moreover, measured and simulated ground vibration velocities are shown in Fig. 9. It can be seen that both peak value and energy-averaged vibration level are very similar, which means the modeling in Sections 3.1 and 3.2 is reasonable and the dynamic model for the monument can be used to predict the vibration responses.

4 Numerical results

In this section, some numerical results will be discussed. As the vibration responses caused by two trains coming across the station at the same time are larger than that caused by just one train operating at one time, all the results shown below are induced by two trains, taking into account the worst operation condition, in terms of vibration effects.

4.1 Mode analysis and response of building

The first four natural frequencies and the related mode shapes numerically obtained from a modal analysis are shown in Fig. 10. It can be seen that all the first four natural frequencies are very low (<5 Hz), and the mode shapes show that the body is more flexible than the foundation of the monument.

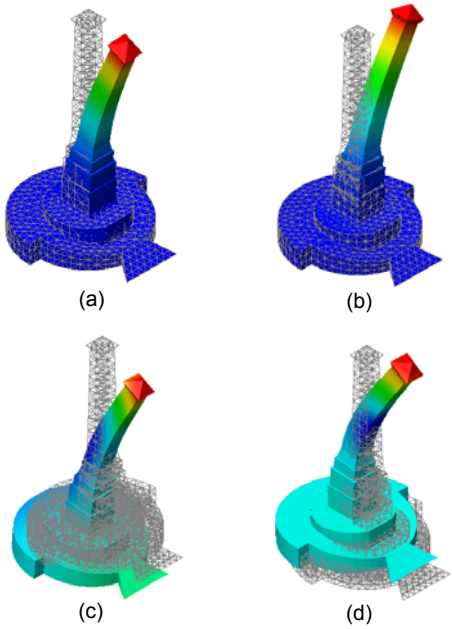

Fig. 10 The first four mode shapes and related natural frequencies of the building
(a) f_1=1.46 Hz; (b) f_2= 1.49 Hz; (c) f_3=1.75 Hz; (d) f_4=2.13 Hz

Fig. 11 describes the response transfer ratio of the building caused by train vibrations, defined as the velocity ratio of the top (Point 0) and bottom (Point 1) in one-third octave band. Between 8 and 80 Hz, the ratio is always larger than one in both horizontal (x-direction) and vertical (z-direction) directions. Vibrations will be enlarged from Point 1 to Point 0 in these frequencies. At frequencies below 5 Hz, the ratio is smaller than one in vertical direction; however, it is very large (even up to 20) in horizontal direction, which means train-induced vibrations can easily cause resonance at low frequencies.

4.1 Dynamic response with different fasteners

It is an effective isolation method that designs different kinds of vibration absorption fasteners. Three kinds of fasteners will be studies here, all of which are widely used in subway track design. The first one, DTVI2 fastener, is typical of the high resilience direct fixation fasteners (Ding, 2010). It is usually directly installed on short sleepers (Fig. 12a). The second kind of fastener is the shearing vibration absorption fastener (Fig. 12b). Generally, this type of fastener possesses double stiffness and good vibration reduction capacity. The last one is Pandrol Vanguard fastener (Fig. 12c), which was initially developed for the British Rail. The elastic wedges are held in place of side bracket which are fastened to the track foundation. The low vertical stiffness gives improved attenuation of the dynamic forces generated at the wheel/rail interface, reducing the level of dynamic forces transmitted through the fastener and into the supporting structure.

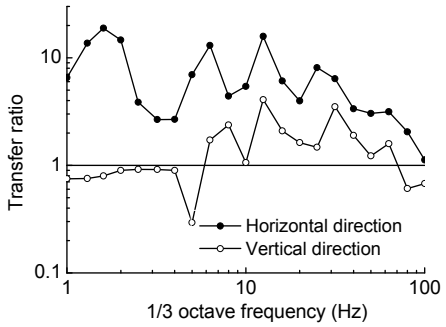

Fig. 11 Transfer ratios of the top and bottom of the building

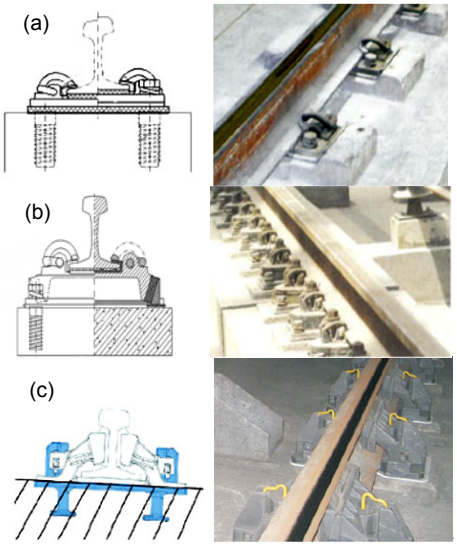

Fig. 12 Sketches (left) and pictures (right) of three kinds of fasteners
(a) High resilience direction fixation fastener; (b) Shearing vibration absorption fastener; (c) Vanguard fastener

All three fasteners have a supporting interval of 0.6 m. The type of rail is UIC-60, which has a cross section area of 7.725×10^3 m^2, a mass per unit length of 60.64 kg/m, and a bending stiffness of 6.434×10^6 N·m^2. The stiffness of the rail pads of DTVI2 fastener is 7.8×10^7 N/m. The track damper fastening model III is chosen as a typical shearing vibration absorption fastener, whose equivalent stiffness is about 1.0×10^7 N/m. The equivalent stiffness of Vanguard fastener is 4.2×10^6 N/m (Jia, 2009).

The time history of the dynamic train loads and horizontal velocities at Point 1 are shown in Fig. 13. It can be seen that, decreasing the stiffness of fastening system is a good way to promote vibration absorption, especially at the vibration sources. Compared with DTVI2 fastener, the other two are effective in attenuating vibrations.

Fig. 14 describes the RMS velocities in horizontal direction at Point 1. Compared with the

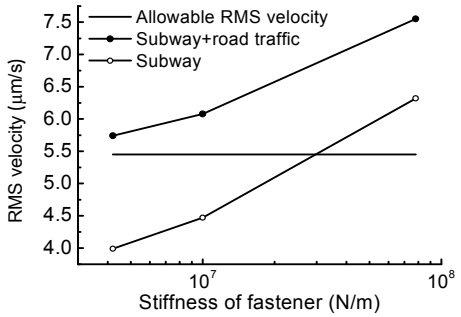

Fig. 14 Dynamic response with different kinds of fasteners

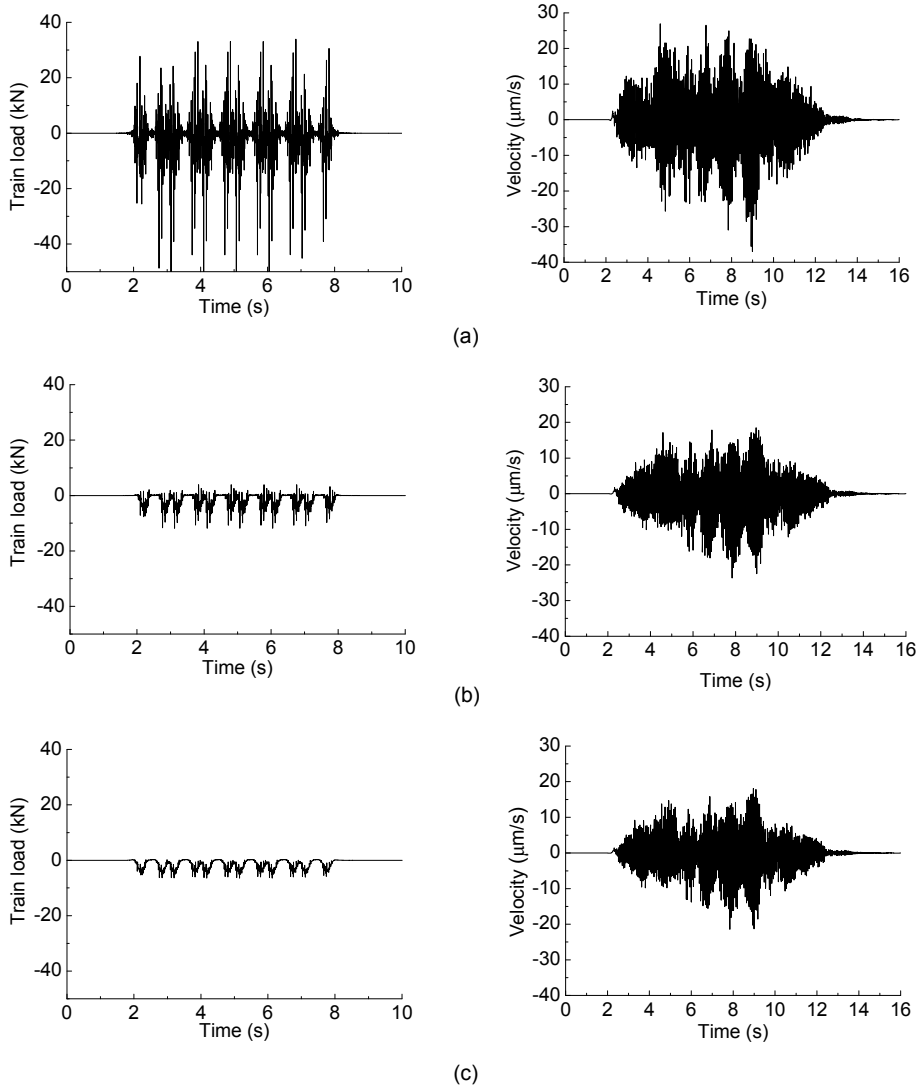

Fig. 13 Dynamic train loads of different kinds of fasteners (left) and horizontal velocity responses at Point 1 (right)
(a) DTVI2 fastener; (b) Model III fastener; (c) Vanguard fastener

allowable RMS velocity, which was 5.45–11.11 μm/s defined in Section 2.2, vibrations induced only by trains could be satisfactory when low-stiffness fasteners are used.

As the square of RMS velocity stands for the vibration energy, Eq. (8) is used to calculate total environmental vibrations with a vibration superposition caused by both road traffic and metro trains.

$$v_{\mathrm{rms,t}} = \sqrt{v_{\mathrm{rms,r}}^2 + v_{\mathrm{rms,m}}^2}, \tag{8}$$

where $v_{\mathrm{rms,t}}$ is the total environmental vibration velocity with the form of RMS, $v_{\mathrm{rms,r}}$ is the RMS velocity mainly induced by road traffic and $v_{\mathrm{rms,m}}$ is the RMS velocity induced by metro trains with the worst potential operation condition in terms of vibration. By site measurement the $v_{\mathrm{rms,r}}$ in horizontal direction at Point 1 is 4.1266 μm/s (Table 1). Comparing the superposition response and allowable RMS velocity, one sees that, due to the contribution of road traffic, all the total vibrations exceed the lower limit, no matter what kind of fastener is used.

In theory, vibration responses would be reduced if the fastener with lower stiffness is used. However, there should be appropriate stiffness relationships between the wheel and track system, or wheel/rail wear or corrugation will develop.

4.2 Dynamic response with different train speeds

Another way to attenuate vibrations is slowing down the train speeds. Some studies have shown that increased train speed will generate a higher dynamic load, and a doubling of the speed will increase the vibration levels by about 4–6 dB, and vice versa (Kurzweil, 1979; Remington and Kurzweil, 1987).

Here five train speeds are studied from 43 to 72 km/h. The stiffness of the fastener is 7.8×10^7 N/m (DTVI2 fastener). Figs. 15 and 16 show the dynamic train loads and RMS velocities in the horizontal direction at Point 1 with five different train speeds.

It can be seen that reducing train speeds produces effective vibration attenuation, both for the train loads at source and the response of structures. The RMS velocities decrease sharply with the train speed, from 65 to 58 km/h. When the train speed is lower than 58 km/h, vibrations are lower than allowable value even if the contribution of road traffic is considered.

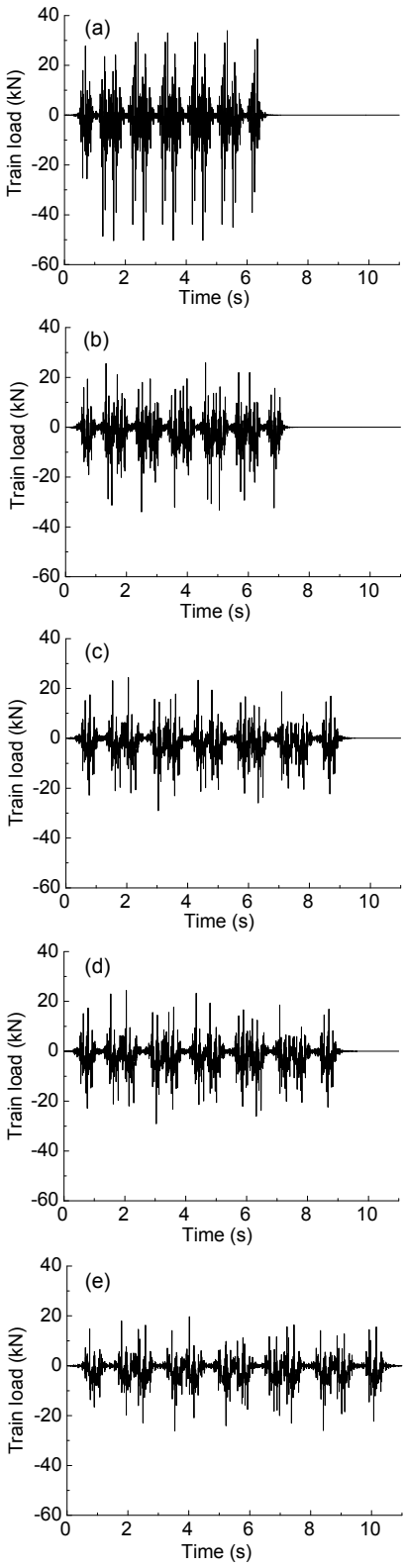

Fig. 15 Train loads with different train speed
(a) 72 km/h; (b) 65 km/h; (c) 58 km/h; (d) 50 km/h; (e) 43 km/h

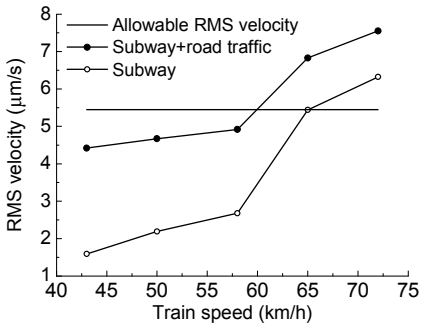

Fig. 16 Dynamic response with different train speeds

5 Conclusions

To protect buildings against long-term traffic vibration, both structural damage and architectural damage should be taken into account, especially for important historic buildings. A primary objective of this paper is to predict the vibration response on the monument in Chengdu due to road traffic and railway trains. The following conclusions have been drawn from the above analyses.

1. According to the vibration criteria listed in GB/T 50452-2008 and the analysis of mode and crest factor, the allowable RMS velocity at the foundation of the monument has been calculated as 5.45–11.11 μm/s, which is a very strict limit for this important structure.

2. A measurement at the monument shows that existing ambient vibrations are lower than the allowable value, but will contribute considerably to the final traffic vibration response.

3. A dynamic train-track model and 3D tunnel-soil-structure FE models have been set up to predict the vibrations at the foundation of the monument. Similar models have been built for Beijing Subway Line 5, and the site measurements at Line 5 have been performed both at the source and ground. A comparison of the acceleration on the rail and the velocity on the ground shows that a good qualitative agreement has been obtained, especially in the time history.

4. Three types of fasteners were considered in the track model. Although the vibrations attenuate a lot when the track damper fastening model III and Vanguard fastener are used, the superposition RMS velocities still exceed the lower limit of allowable value.

5. Five different train speeds were considered. Results show that reducing train speeds leads to effective vibration attenuation. The RMS velocities decrease sharply with the train speed from 65 to 58 km/h. When the train speed is lower than 58 km/h, vibrations are lower than allowable value even if the contribution of road traffic is considered.

References

Bata, M., 1971. Effects on buildings of vibrations caused by traffic. *Building Science*, **6**(4):221-246. [doi:10.1016/0007-3628(71)90014-4]

Bazaco, M., Montoya, F., Alvarez, V., Arroyo, F., Arnaiz, S., 1995. Traffic induced vibrations in historic buildings. Case of study: Palacio de Sta. Cruz of Valladolid. *WIT on Built Environment*, **15**:109-118.

Chiostrini, S., Marradi, A., Vignoli, A., 1995. Evaluation of traffic-induced vibrations in historic buildings: the case of the "Galleria Vasariana" in Florence. *WIT on Built Environment*, **17**:69-76.

Clemente, P., Rinaldis, D., 1998. Protection of a monumental building against traffic-induced vibrations. *Soil Dynamics & Earthquake Engineering*, **17**(5):289-296. [doi:10.1016/S0267-7261(98)00012-8]

Crispino, M., D'Apuzzo, M., 2001. Measurement and prediction of traffic-induced vibrations in a heritage building. *Journal of Sound & Vibration*, **246**(2):319-335. [doi:10.1006/jsvi.2001.3648]

Ding, D.Y., Gupta, S., Liu, W.N., Lombaert, G., Degrande, G., 2010. Prediction of vibrations induced by trains on line 8 of Beijing metro. *Journal of Zhejiang University SCIENCE A (Applied Physics & Engineering)*, **11**(4):280-293. [doi:10.1631/jzus.A0900304]

Ellis, P., 1987. Effects of traffic vibration on historic buildings. *Science of The Total Environment*, **59**(4):37-45. [doi:10.1016/0048-9697(87)90429-3]

Esveld, C., Markine, V.L., 2006. Assessment of high-speed slab track design. *European Railway Review*, **12**(6):55-62.

GB/T 50452-2008. Technical Specifications for Protection of Historic Buildings Against Man-Made Vibration. China Building Industry Press, Beijing (in Chinese).

Grassie, S.L., 1984. Dynamic Modelling of Railway Track and Wheelsets. Proceedings of the 2nd International Conference on Recent Advances in Structural Dynamics, Southampton, p.681-698.

Heckl, M., Hauck, G., Wettschureck, R., 1996. Structure-borne sound and vibration from rail traffic. *Journal of Sound & Vibration*, **193**(1):175-184. [doi:10.1006/jsvi.1996.0257]

Jia, Y.X., 2009. Study on Analytical Model of Coupled Vehicle & Track and Effect to Environment by Metro Train-Induced Vibrations. PhD Thesis, Beijing Jiaotong University, Beijing, China (in Chinese).

Jia, Y.X., Liu, W.N., Liu, W.F., Zhang, H.G., 2008. Study of Vibration Effects on Historic Buildings Due to Moving

Trains in Beijing. 9th International Symposium on Environmental Geotechnology and Global Sustainable Development, Hongkong, p.492-499.

Kok, A.W.M., 1995. Lumped Pulses and Discrete Displacements. PhD Thesis, Delft University of Technology, Delft, the Netherlands.

Kurzweil, L.G., 1979. Ground-borne noise and vibration from underground rail systems. *Journal of Sound and Vibration*, **66**(3):363-370. [doi:10.1016/0022-460X(79)90853-8]

Lei, J., Zhao, C.H., He, X.D., Yuan, M.W., 2009. A Study on Mitigating Environment Vibration Hazards in Metropolis. 5th Association of Pacific Rim Universities Research Symposium, Taipei, p.44-45.

Liu, W.F., Liu, W.N., Jia, Y.X., Zhang, H.G., 2007. Study on Effect on Ming Dynasty's City Wall Due to Train Induced Vibration's in Beijing. 3nd International Symposium on Environmental Vibration, Taipei, p.229-234.

Ma, M., Liu, W.N., Ding, D.Y., Sun, X.J., 2009. Vibration Impacts on Adjacent Heritage Buildings Induced by Metro Trains. 4th International Symposium on Environmental Vibration, Beijing, Science Press, China, p.394-399.

Markine, V.L., Esveld, C., 2007. Assessment of High-Speed Slab Track Design. Proceedings of the Eleventh International Conference on Civil, Structural and Environmental Engineering Computing, Civil-Comp Press, Stirlingshire, UK.

Markine, V.L., de Man, A.P., Toropov, V.V., Esveld, C., 2000. Optimization of Railway Structure Using Multipoint Approximations Based on Response Surface Fitting (MARS). Proceedings of the 8th AIAA/USAF/NASA/ISSMO Symposium on Multidisciplinary Analysis and Optimization, Long Beach, California.

Markine, V.L., Zwarthoed, J.M., Esveld, C., 2001. Use of Numerical Optimisation in Railway Slab Track Design. Proceedings of the 3rd ASMO UK/ISSMO Conference, North Yorkshire, UK.

Markine, V.L., de Man, A.P., Esveld, C., 2003. Identification of Dynamic Properties of a Railway Track. Proceedings of the IUTAM Symposium on Field Analyses for Determination of Material Parameters-Experimental and Numerical Aspects, Kiruna, Sweden.

Pau, A., Vestroni, F., 2008. Vibration analysis and dynamic characterization of the Colosseum. *Structural Control and Health Monitoring*, **15**(8):1105-1121. [doi:10.1002/stc.253]

Remington, P.J., Kurzweil, L.G., 1987. Low-Frequency Noise and Vibrations from Trains. Nelson, P.M. (Ed.), Transportation Noise, Butterworth & Co. Ltd., London.

Sanò, T., de Sortis, A., Rinaldis, D., 1998. Experimental and Numerical Study on Traffic-Induced Soil Vibrations. International Conference on Noise and Vibration, Leuven, Belgium.

Steenbergen, M.J.M.M., 2008. Wheel-Rail Interaction at Short-Wave Irregularities. PhD Thesis, Delft University of Technology, Delft, the Netherlands.

Wang, J.W., 2006. Testing study on Dynamic Properties of Sand Pebble Soil in Sichuan. MS Thesis, Southwest University of Science and Technology, Mianyang, China (in Chinese).

Zhang, C.Y., 2002. The analysis of rock mass fatigue effect under vibration environment in Luoyang Longmen Grottoes. *Acta Scientiarum Naturalium Universitatis Pekinensis*, **38**(6):809-816 (in Chinese).

Zienkiewicz, O.C., Taylor, R.L., 1988. The Finite Element Method (4th Ed.). Mc Graw Hill, London.